

# Strategic modeling for diagnosis and annihilation of cancer cells with nanobubbles developed from multimode fiber optic based plasmonic nanosensors

Saikat Das

Department of Physics and Mathematics, University of Eastern Finland, Finland  
[saikatshiva@gmail.com](mailto:saikatshiva@gmail.com)

**Abstract:** We address a pioneering approach of cancer treatment based on vapor nanobubbles developed from multimode optical fibers. The optical fibers can be utilized for sensing applications like detection of pathogens, sensing of chemical and biological species etc. and at the same time can be used for the detection and remedy of cancer. The procedure starts with the theoretical simulation of the optical fiber plasmonic sensors. Then these nanosensors are fabricated and their sensitivities measured experimentally. The nanobubbles technique of cancer treatment deploys etching of metal nanoparticles from the metal layer of the optical fibers and then instigating the nanospheres by laser pulse(s) to form nanobubbles. The intensities of the scattering signals by the nanobubbles surrounding the cancerous cells would be higher than those of normal cells which help in detecting cancer cells. After detection of cancer cells, the energies of the laser pulses are increased which help in increasing the lifespan and volume of the nanobubbles. The nanobubbles swell up to obliterate the chromosomal materials of the cancerous cells.

**Keywords:** Optical fibers, Plasmonics, Nanosensors, Cancer, Nanobubbles.

## 1. Introduction

Day by day, Cancer is outreaching its poisonous claws in our lives as death sentence for us. There is no distinct test that can explicitly detect cancer. The detection of cancer customarily demands a detailed physical check-up of a patient along with several indicative tests in the laboratory. The commonly used detection techniques for cancer are X-rays biopsy, magnetic resonance imaging, computed tomography scan, blood tests, endoscopy, surgery etc. [1]. For example, biopsy is carried out to cut out cells from the body for the purpose of medical examination. But this tumor biopsy test is among the most fallacious of all laboratory tests and is susceptible to erroneous findings. The first error is overdiagnosis-when the test results of a patient turn out positive but the patient actually does not have cancer. The mirror image of overdiagnosis is underdiagnosis-when a patient genuinely has cancer but does not spell out positive results [2, 3].

Regarding cancer treatment, the most commonly used procedure at present is chemotherapy. Chemotherapy [4] is a systemic therapy, which means that it acts on the whole body by passing through the blood. Chemotherapy drugs target rapidly dividing cells. As cancer cells grow uncontrollably faster than normal cells, chemotherapy drugs can mutilate cancer cells. But some normal cells in our body such as mouth, bone marrow, intestinal tract, hair follicles, nails, and vagina also divide rapidly [5]. Thus chemotherapy drugs act on them, too. On the other hand, dosimetry i.e. the correct dosage of medicine plays a pivotal role in chemotherapy. If the dosage is low, the cancer cells are not fully destroyed and they recur again. So, it is not enhancing mortality, only survival [2]. If the dosage is very high, it becomes deadly for the patients.

This article evolved out of the attempt to answer the question that the hostility of cancer can be ever encountered. Our proposed technique of cancer detection and treatment by plasmonic nanobubbles developed from plasmonic nanosensors utilizes only light and heat energies which are absolutely natural to living bodies. The nanobubbles can scrupulously annihilate the cancerous cells without affecting the adjoining normal cells. So there is much less side-effect as compared to chemotherapy. Two characters stand at the focus of this technique. The first is Plasmonics, one of the most marvellous fields of Physics. The second is Cancer, the defining anathema of this generation.

The aim of this study is to develop some nanosensors based on the phenomenon of surface plasmon resonance, which can act not only as sensors but also for the detection and remedy of cancer. So, the target of our study can be divided into two parts.



## 2. Development of the plasmonic nanosensors

In the first part, we will discuss about the development of the plasmonic nanosensors. We know that the phenomenon of surface plasmon resonance can take place at metallic interfaces. So, we selected an interface, one side of which is a metal and the other a dielectric. In our study, we took optical fibers as the base medium of the nanosensors. The reason behind the selection of optical fibers as the base medium of nanosensors was that we wanted to use the same nanosensors for treatment of cancer and that the technology of fiber optics would serve the purpose of transfer and guidance of nanobubbles based cancer treatment.

At first we carried out theoretical simulation for optical fibers and using argon-ion laser as the light source in MATLAB program. The condition of surface plasmon resonance at metal-dielectric interface depends on: (i) Angle of incidence of light, (ii) Wavelength of light beam, (iii) Dielectric functions of metal and dielectric [6]. Keeping metal (silver) and dielectric (air) fixed, we first selected a particular wavelength of the argon-ion laser and then found out the theoretically simulated value of the surface plasmon resonance angle. This technique is called angular interrogation [6, 7]. We repeated this process for nine different wavelengths of argon-ion laser and obtained nine corresponding values of surface plasmon resonance angle.

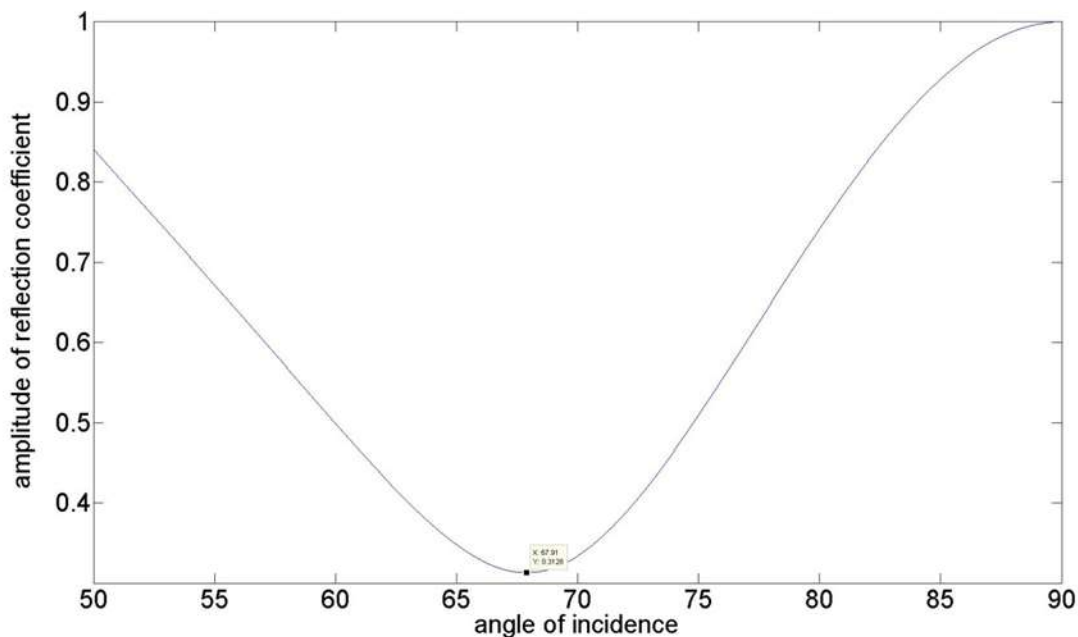
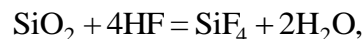


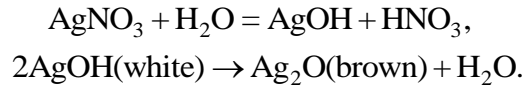
Fig. 1. Surface plasmon resonance curve obtained after theoretical simulation of the nanosensor corresponding to 454 nm wavelength of argon-ion laser.

After theoretical simulation, the process of chemical deposition of silver layer on the fiber optic SPR sensors was carried out. The optical fiber that was taken as sample was a multimode optical fiber (core diameter: 50  $\mu\text{m}$ , cladding diameter: 125  $\mu\text{m}$ ). The length of the optical fiber was 10 cm. Firstly, the Teflon jacket was removed from the optical fiber by dipping the fiber in acetone solution for about 20 minutes. Next, a solution was prepared by mixing HF (48%) and distilled water in the ratio of 1:2 by volume and the middle portion of the optical fiber was dipped in that solution which resulted in the removal of cladding from the immersed portion of the fiber.



After this, the sample (unclad optical fiber) was washed with 5%  $\text{SnCl}_2$  solution which was prepared by mixing 2.5 grams of  $\text{SnCl}_2$  with 50 c.c. of distilled water. It helped in the binding of silver to the sample surfaces. In the next step, 5 grams of  $\text{AgNO}_3$  was taken and mixed with 50 c.c. of distilled water. It resulted in the formation of  $\text{AgOH}$  (white) which further decomposed to yield  $\text{Ag}_2\text{O}$  (brown) and water.

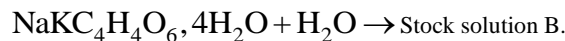




Then, 50 c.c. of  $\text{NH}_4\text{OH}$  solution was taken and diluted with 100 c.c. of distilled water. After this, the  $\text{NH}_4\text{OH}$  solution was mixed with  $\text{Ag}_2\text{O}$  solution to yield a clear solution of Argento ammonium hydroxide[8]. This solution is the stock solution A.



Next, 70 grams of Sodium potassium tetrata (  $\text{NaKC}_4\text{H}_4\text{O}_6, 4\text{H}_2\text{O}$  ) was mixed with 100 c.c. of distilled water to give stock solution B.



Then, the stock solution B was mixed with stock solution A and heated to  $50^\circ\text{C}$  temperature. Then, we had silver deposition on the surface of the beaker. A slight stirring facilitated the deposition. Next, we placed our experimental samples in the beaker to get silver layer deposited on the surface of the samples. So, we obtained multimode optical fibers coated with silver layer which are further surrounded by a dielectric sensing medium (at first air and then turpentine). Then, we used Ferric nitrate  $\text{Fe}(\text{NO}_3)_3$  to etch out the deposited silver from the ends of the optical fibers. Next, when inspected under microscope, it was found out that the silver layer had been deposited almost uniformly over the core of the optical fiber.



Fig. 2. Microscopic (40X, N.A. 0.65) image of silver layer deposited on the surface of the unclad multi-mode optical fiber. The silver layer deposited over the core of the optical fiber was found out to be substantially uniform.

After this, we measured the intensity reflectance through the nanosensor as a function of the angle of incidence of light beam. Keeping wavelength constant, if angle of incidence of light beam is varied, then a sharp dip appears at a particular angle, which we call resonance angle. This process was then repeated for different wavelengths. We used a CVI Melles Griot argon-ion laser (Model: 35-LAP-431-230; Serial No.: 2985-T) as the light source. Argon-ion lasers produce many wavelengths in the violet-green spectral region. Nine different wavelengths were utilized in this experiment. They were chosen individually by Fabry-Perot interferometer. The polarizer was employed to obtain p-polarized light which actually kindles the excitation of electron density oscillations (called surface plasmon wave) at metal-dielectric interface, thereby facilitating the phenomenon of surface plasmon resonance. The lens of focal length 16 mm was used as a collimator. The sample i.e. optical fiber was placed on a rotating goniometer (angle of resolution =  $0.001^\circ$ ) which allowed the sample to be rotated to a specific angular position, thereby assisting us to vary the angle of incidence of laser beam. The position of the detector depends on the direction of the reflected light through the nanosensors, which in turn, depends on the angle of incidence of the laser beam. As we know that the nanosensor used is of short length, it is subject to instability and hence variations in the transmitted intensity of the radiation, if the nanosensor is not mechanically stable when using the goniometer. This problem was overcome by giving the transmitted intensity of the radiation enough time to become stable after each rotation.



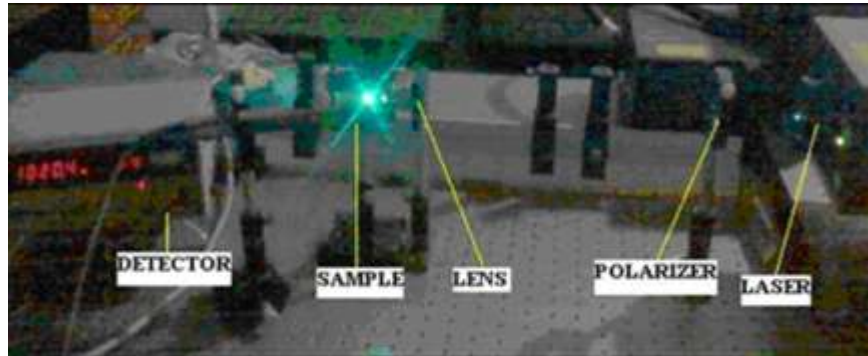


Fig. 3. Experimental set-up for measuring the intensity reflectance through the nanosensor as a function of angle of incidence of light beam.

Table I illustrates the theoretically simulated and experimentally obtained values of SPR angle for the nanosensor corresponding to nine different wavelengths of Ar-ion laser.

Table I. Comparison of theoretically simulated and experimentally obtained values of SPR angle corresponding to nine different wavelengths of Ar-ion laser.

Wavelengths	SPR angles (theoretical)	SPR angles (experimental)
454 nm	67.9°	64.9°
458 nm	67.7°	64.6°
465 nm	67.5°	64.4°
472 nm	67.3°	64.2°
477 nm	67.2°	64.0°
488 nm	66.9°	64.0°
496 nm	66.7°	64.0°
502 nm	66.5°	63.7°
514 nm	66.1°	63.5°

### 3. Sensing properties of the plasmonic nanosensors

A metal-dielectric interface advocates charge density oscillations along the interface which are designated as surface plasma oscillations and quantum of these oscillations is called surface plasmon. The evanescent wave instigates the surface plasmons at the metal-dielectric interface. Fig. 4 illustrates the schematic representation of a fiber optic surface plasmon resonance based sensor.

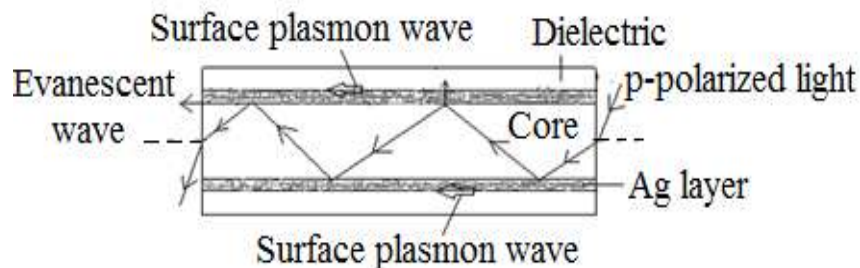


Figure 4: Schematic diagram of a fiber optic surface plasmon resonance based sensor.



When the evanescent wave with a propagation constant equal to that of the surface plasmon wave is incident on the metal dielectric interface, resonance occurs. Now Fig. 5 illustrates how a change in refractive index of the sensing layer i.e. dielectric ( from air,  $n_s = 1$  to turpine oil,  $n_s = 1.47$  ) results in a change of the surface plasmon resonance angles for the nanosensor respectively.

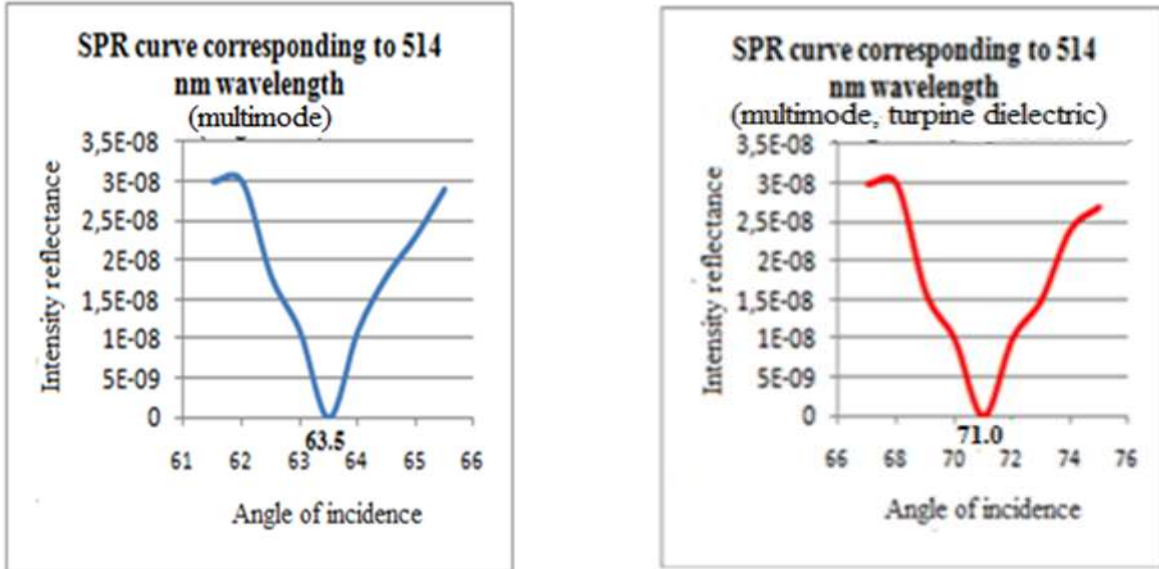


Fig. 5. Comparative analysis of surface plasmon resonance curves obtained experimentally for multimode optical fibers (left) with air as dielectric, (right) with turpine oil (1.47) as dielectric.

From Fig. 5 (right), we see that after changing the dielectric from air to turpine oil ( $n_s = 1.47$ ), when the performance of the nanosensor was analysed again using Ar-ion laser at 514nm, the SPR angle shifted from  $63.5^\circ$  (for air) to  $71.0^\circ$  (for turpine oil). The sensitivity [6] of the nanosensor is calculated as the deviation in the value of the resonance angle  $\delta\theta_{res}$  with a change in the refractive index  $\delta n_s$  of the dielectric layer and is given by

$$S_n = \frac{\delta\theta_{res}}{\delta n_s} \quad (1)$$

Employing the above formula, the sensitivity of the nanosensor was found to be 0.27.

The accuracy [9] of the goniometer measurements depend on the uncertainty of the measurements executed with the instrument. The following definition is used to evaluate the uncertainty value for a given set of measurements. Let us assume that a number of

measurements  $N$  of an angle 'a'  $a_1, a_2, a_3, \dots, a_N$  be taken. The mean value  $\bar{a}$  of the measurements is:

$$\bar{a} = \frac{a_1 + a_2 + a_3 + \dots + a_N}{N} \quad (2)$$

The standard deviation  $\sigma_a$  of the measurements is:

$$\sigma_a = \sqrt{\frac{1}{N-1} \sum_1^i (a_i - \bar{a})^2} \quad (3)$$

and the uncertainty  $\sigma_a$  is:



$$\sigma_a = \frac{\sigma_a}{\sqrt{N}}, \quad (4)$$

Table II illustrates the nine angular measurements that were taken with the goniometer and the uncertainty value. The actual uncertainty calculated with Equ. 4 is  $0.1^\circ$ . Mean Square for treatments follows the common practice of multiplying it by 2 to enhance the level of confidence on the uncertainty. Therefore the value given is  $0.2^\circ$ .

Table II. Nine angular measurements taken with the goniometer and the uncertainty value.

Measurements	Angles
1	$64.9^\circ$
2	$64.4^\circ$
3	$64.6^\circ$
4	$64.2^\circ$
5	$64.0^\circ$
6	$64.0^\circ$
7	$64.0^\circ$
8	$63.7^\circ$
9	$63.5^\circ$
Average:	$64.1^\circ$
Standard deviation:	$0.4^\circ$
Uncertainty ( $\times 2$ )	$0.2^\circ$

To summarize, when we are saying that the value of the SPR angle obtained experimentally is  $64.9^\circ$ , the actual angle could have any value between  $65^\circ$  and  $64.8^\circ$ . Our following task was to use the same nanosensors for diagnosis and healing of cancer. This can be looked upon as the second section of our analysis.

#### 4. Strategy for development of metal nanoparticles from metal layer by chemical etching technique

Silver nanoparticles can be tailored out from the deposited silver layer by chemical etching technique. Fig. 6 illustrates the schematic diagram of the experimental set-up that can be used for the purpose of chemical etching.

At first, an etchant solution is to be prepared. The container containing the etchant solution must be cooled by ice. The outlet pipe from the container is equipped with a valve which will allow us to control the flow of the etchant solution. It is followed by a pressure gauge which can measure the liquid pressure before the etchant solution can enter the constricted or compressed channel. The compressed channel has a wider entrance orifice and a narrower exit orifice. When the etchant solution is compelled to enter the channel having such wider entrance orifice and narrower exit orifice, it results in a remarkable increase in pressure, which impedes the motion of the etchant solution inside the channel. Plates with pores of multifarious shapes can be used as the base plate of the compressed channel. The base plate of the channel is provided with pores which will allow the etching of the silver layer in contact with the base plate. The channel is placed atop the fiber optic SPR-based sensor so that the silver layer comes in contact with the base plate of the constricted channel and etching takes place.

The nanoparticles are carved out by changing the base plate of the channel after a certain time-interval and also controlling the flow of the etchant solution by the valve. The etchant solution is recycled back into the container by a pump so that it can be used once more. The pipes must be made of acrylic material, which are immune to etching or corrosive reaction of the etchant solution.



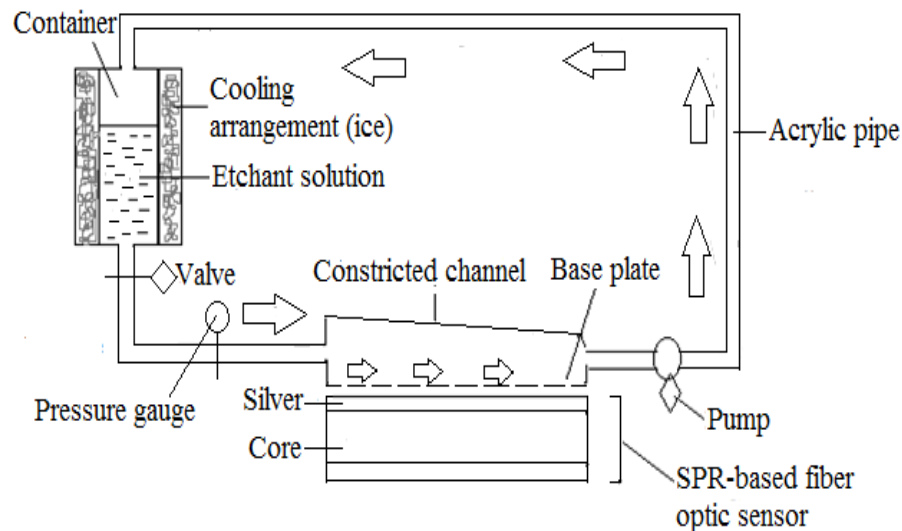


Fig. 6. Schematic diagram illustrating the set-up used for chemical etching of nanoparticles.

## 5. Plasmonic nanobubbles

For the development of plasmonic nanobubbles, noble metal nanoparticles can be assorted in batches to form nanoparticle clusters. The nanoparticle clusters are then activated by single or multi-wavelength laser pulse to give rise to plasmonic nanobubbles. The optical energy catered by the laser pulse(s) is transformed into heat energy by surface plasmon resonance. This heat energy is then picked up by the surroundings of the nanoparticle-clusters which becomes responsible for vaporization of the surroundings. This vapour form is ultimately enlarged to give rise to plasmonic nanobubbles encompassing the metal nanoparticle-clusters. This is the general technique of germination of nanobubbles which exploits one surface plasmon resonance as the source of heat [10, 11].

## 6. Strategic modelling for diagnosis of cancer cells

Based on the technique of formation of plasmonic nanobubbles, we will figure out two slightly different arrangements—one for diagnosis of cancerous cells and another for annihilation of cancerous cells. Fig. 7 illustrates the schematic diagram for the detection of cancer cells. A dual-pulsed laser providing two different pumping laser pulses simultaneously can be used as the light source. It is followed by a polarizer to get p-polarized light and then by a lens to collimate the light beams. Then these dual laser pulses are allowed to enter the multimode fiber optic based nanosensors through one of its endfaces. The laser pulses then cause excitation of electron density oscillations (called surface plasmon wave) at metal-dielectric interface. The optical energy furnished by the dual laser pulses is transformed into heat energy by surface plasmon resonances. This heat energy is then tapped by the surroundings of the Au nanoparticle clusters which helps in vaporization of the surroundings. This vapour form starts increasing in size to give rise to plasmonic nanobubbles circumscribing the nanoparticle-clusters. The cells (both cancerous as well as normal) are placed on metal-dielectric interface. Then, a supplementary probe beam of wavelength different from the pumping laser pulses, is aimed at the cells. The nanobubbles developed around the cells as well as the cells themselves scatter a part of this probe beam. The intensities of the scattering signals for cancerous and normal cells are measured by a photodetector (photodetector 1) placed perpendicularly to the axis of the optical fiber. The axial intensity of the probe laser beam coming out of the metal-dielectric interface is measured by another photodetector (photodetector 2). Here, the energies of the pumping laser pulses should be selected such that their combined total is much below the energy level that can favor the lifespan of the nanobubbles for cell damage level. In Fig. 7, the green and violet arrows represent the multi-wavelength pumping laser pulses while the red arrows represent the additional probe laser beam. We know that the cancer cells share one common feature: abnormal growth. The cancer cells are gigantic in size as compared to the normal cells. So the intensities of the scattering signals as measured by photodetector 1 for the cancer cells will be much higher than those for normal cells. On the other hand, the axial intensities of the probe beam as measured by photodetector 2 for the cancer cells will be feeble as compared to the normal cells.



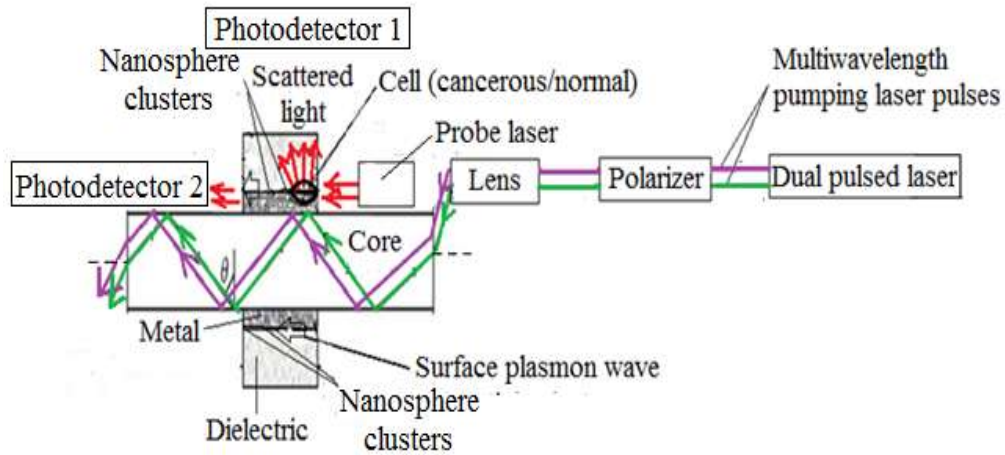


Fig. 7. Schematic diagram illustrating the technique for detection of cancer cells.

**7. Strategic modeling for annihilation of cancer cells**

After we can distinguish the cancerous cells from the normal ones, we will discuss about the set-up for annihilation of the cancerous cells. Fig. 8 represents the schematic diagram illustrating the arrangement for destruction of the cancerous cells. The destruction of the cancerous cells by nanobubbles is conceived by increasing the energy of the pumping laser pulses (wavelengths remaining same) such that their sum-total is higher than the energy level that favor the lifespan of the nanobubbles for cell damage. Higher the energies of the pumping laser pulses, greater will be the amount of heat energy available for formation of nanobubbles which indicates an increase in the spatial dimensions as well as the lifespan of the nanobubbles. So, the nanobubbles will start expanding in size. In order to occupy a larger volume, these nanobubbles will then rupture the cell membranes of the cancerous cells and destroy the chromosomal materials of the malignant cells. Unlike detection technique, no extra probe laser is used here. The damage of the cancerous cell is conformable to the increased spatial dimensions (or in other ways, lifespan) of the nanobubbles. The annihilation of the malignant cancerous cells can be carried out in an environment comprising of both cancerous as well as normal cells. So, whenever a cancerous cell is detected, we increase the energy of the pumping laser pulses which becomes responsible for destruction of the cancerous cell. But when a cell is found to be normal, we always maintain the energies of the pumping pulses such that their combined total is much below the energy level that can favor the lifespan of the nanobubbles for cell damage level. So, the cancerous cells can be destroyed while the adjoining normal cells will remain unaffected.

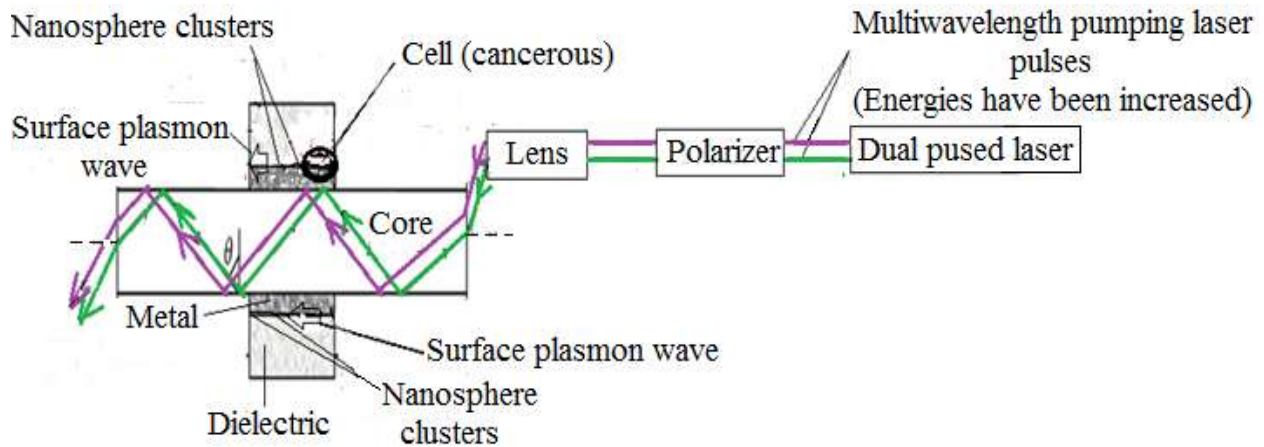


Fig. 8. Schematic diagram illustrating the technique for annihilation of cancer cells.



## 8. Conclusions

In conclusion, we developed multimode fiber optic based plasmonic nanosensors, which can act not only as sensors but also can be used for the detection and remedy of cancer. The plasmonic nanosensors have sensing properties and can be used in sensing applications like detection of pathogens, sensing of chemical and biological species etc. The nanobubbles technique employs etching of metal nanospheres from the metal layer of the optical fibers and then instigating the nanospheres by laser pulse(s) to form nanobubbles. It has very good selectivity in destruction of cancerous cells only and not affecting the circumscribing normal cells. But in chemotherapy, the most commonly used technique for treatment of cancer, normal cells are also greatly affected which leads to many adverse side-effects and sometimes the vital organs in our body are also greatly affected. In chemotherapy, drugs are used for destruction of the malignant tumors which have many side-effects. Dosage of chemotherapy is also extremely difficult. If it is very low, then cancer recurs and if it is very high, the level of toxicity becomes lethal to the patients. There is no such risk or side-effect in this technique. Hence, the plasmonic nanobubbles can be recognized as a cutting-edge technology for detection and annihilation of cancer. *In vitro* and *in vivo* experimental analysis following the set-ups of detection and annihilation of cancer cells would come up in future.

## References

- [1]. D. Cantor, "Introduction: Cancer Control and Prevention in the Twentieth Century," *Bulletin of the History of Medicine* 81, 1-38 (2007).
- [2]. S. Mukherjee, "The Emperor Of All Maladies: A Biography Of Cancer," *New England Journal of Medicine*, Scribner, ISBN: 978-1-4391-0795-9 (2010).
- [3]. A. N. Monteiro and R. Waizbord, "The Accidental Cancer Geneticist," *Cancer Biology and Therapy* 6, 811-813 (2007).
- [4]. S. Ariad and W. R. Bezwoda, "High-Dose Chemotherapy; Therapeutic Potential in the Age of Growth Factor Support," *Israel Journal of Medical Sciences* 28, 377-385 (1992).
- [5]. [http://www.breastcancer.org/treatment/chemotherapy/side\\_effects](http://www.breastcancer.org/treatment/chemotherapy/side_effects)
- [6]. B. D. Gupta and R. K. Verma, "Surface plasmon resonance-based fiber optic sensors: Principle, probe design, and some applications," *Journal of Sensors* (2009), doi:10.1155/2009/979761
- [7]. J. Guo, P. D. Keathley, and J. T. Hastings, "Dual-mode surface-plasmon-resonance sensors using angular interrogation," *Opt. Lett.* 33, 5, 512 (2008).
- [8]. P. W. Atkins, "Physical Chemistry," Oxford University Press, 6th edition, 858-859 (1998).
- [9]. <http://www.microstartech.com/index/NanoindenterAngularMeasurements.pdf>
- [10]. L-Hleb Ekaterina, A. O. Oginsky, A. P. Samaniego, D. L. Shenefelt, D. S. Wagner, J. H. Hafner, M. C. Farach-Carson, D. O. Lapotko, "Tunable Plasmonic Nanoprobes for Theranostics of Prostate Cancer", *Theranostics* 10, (2011).
- [11]. Z. Liu, W. H. Hung, and M. Aykol, "Optical manipulation of plasmonic nanoparticles, bubble formation and patterning of SERS aggregates," *Nanotechnology* 21, 105304 (2010).

